



## STUDY ON THE STRUCTURAL PERFORMANCE OF RECTANGULAR STEEL TUBES

T. Miura<sup>(1)</sup> and T. Fujimoto<sup>(2)</sup>

<sup>(1)</sup> Graduate Student, Graduate School of Industrial Technology, Nihon University, [citm19011@g.nihon-u.ac.jp](mailto:citm19011@g.nihon-u.ac.jp)

<sup>(2)</sup> Professor, Architecture and Architectural Engineering, College of Industrial Technology, Nihon University, [fujimoto.toshiaki@nihon-u.ac.jp](mailto:fujimoto.toshiaki@nihon-u.ac.jp)

### **Abstract**

Currently, in Japan, square cross-sectional steel tubes are generally used as columns in steel buildings such as concrete-filled steel tube (CFT). In recent years, however, the use of rectangular cross-sectional columns has increased in CFT-built buildings with excellent seismic performance. Examples include the use of rectangular cross-sections as outer columns to suppress horizontal displacement due to seismic forces and wind pressure, and the building that column cross-section has been set the rectangle considering the location of the newly planned railroad track. Rectangular CFT columns may be preferred for various reasons, such as structural planning and floor planning, and more rational designs become possible when rectangular steel tubes are used. Rectangular steel tubes are included in the standards of several other countries, but in Japan, experimental data are limited, and the design methods for steel tubes and CFT columns remain unclear. Therefore, experiments on the structural performance of rectangular CFT columns have been widely performed. Based on these experiments, it is known that the width-thickness ratios of both their long and short sides affect the strength and deformation behaviors when rectangular CFT columns are exposed to stress. In this study, the effect of cross-sectional shape on structural performance of the rectangular steel tube was examined. First, the generic performance of the cross section was demonstrated using central compression and eccentric compression tests of the stub-columns. The effect of cross-sectional shape, bending direction, and the presence of axial forces on columns was then examined using monotonic bending tests. The results show that when an axial compression force is applied in isolation, short-side length had no effect on the structural performance.; however, when bending forces were applied, cross-sectional shape greatly affected the maximum strengths and the deformation capacities of the samples.

*Keywords: steel tube; rectangular cross-section; compression test; bending test; width-thickness ratio*



## 1. Introduction

In recent years, there were some examples in Japan where rectangular cross-sections of steel columns were used for concrete-filled tubular (CFT) steel columns. In these cases, the reasons for using a rectangle for the column cross-section include structural and floor planning. There are examples in which a rectangular CFT column is applied only to the outer column to suppress horizontal displacement due to seismic force and wind pressure and an example in which the column is applied to fit in a wall.

Currently in Japan, CFT columns and other steel columns are generally circular or square in cross-section, and the design method for applying rectangular steel tubes remains unclear. Furthermore, there are little experimental data on rectangular steel tubes (CFT and steel columns). In this study, the effect of the cross-sectional shape on the structural performance of the rectangular steel tubes was examined.

## 2. Experimental outline

### 2.1 Specimens and parameters

Figure 1 shows the dimensions of the test specimens. The cross-sections were square and rectangular and

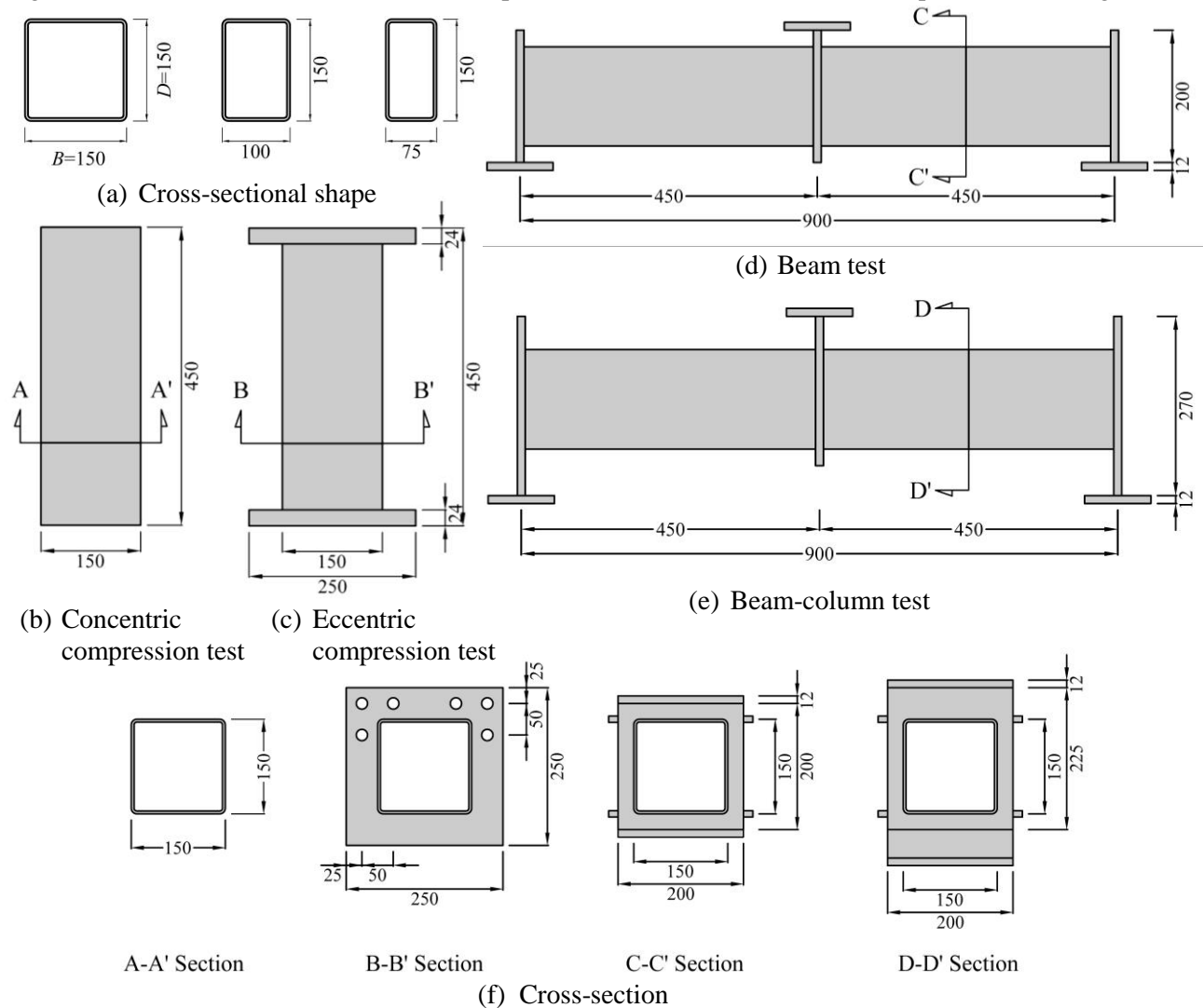


Fig. 1. Dimensions of test specimens



were of three types: 150 mm × 150 mm, 150 mm × 100 mm, and 150 mm × 75 mm shown in Fig. 1(a). The wall thickness of the steel tube ( $t$ ) was unified to 4.5 mm, the specimen length in the compression test ( $L$ ) was three times as long as the cross-section long side (450 mm) shown in Fig. 1(b) and (c), and the distance between fulcrums in the bending test ( $L$ ) was six times as long as the cross-section long side (900 mm) shown in Fig. 1(d) and (e). Table 1 shows specimens and results of the tensile test.

Parameters in the central compression test are cross-sectional. In the eccentric compression test, the parameters are cross-sectional, in the bending direction, and eccentric distance because the rectangular steel tube had a short and long side direction. In the beam and beam-column test, the parameters are cross-sectional and in a bending direction, and the comparisons were made with and without the axial force. The axial force was 20% of the tensile yield strength.

Table 1. Specimen Outline

	Specimen	$B$ (mm)	$D$ (mm)	$t$ (mm)	$L$ (mm)	$\alpha_B$	$\alpha_D$	$\sigma_{cy}$ (Mpa)	$\sigma_{cu}$ (Mpa)
Concentric Compression Test	C0-S150-150	150	150	4.22	450	1.58	1.58	405	484
	C0-R100-150	100	150	4.24	450	1.06	1.60	417	470
	C0-R75-150	75	150	4.16	450	0.81	1.62	414	484
Eccentric Compression Test	E50-S150-150	150	150	4.22	450	1.58	1.58	405	484
	E50-R100-150	100	150	4.24	450	1.06	1.60	417	470
	E50-R75-150	75	150	4.16	450	0.81	1.62	414	484
	E25-R150-100	150	100	4.24	450	1.60	1.06	417	470
	E25-R150-75	150	75	4.16	450	1.62	0.81	414	484
Beam Test	B-S150-150	150	150	4.22	900	1.58	1.58	405	484
	B-R100-150	100	150	4.24	900	1.06	1.60	417	470
	B-R75-150	75	150	4.16	900	0.81	1.62	414	484
	B-R150-100	150	100	4.24	900	1.60	1.06	417	470
	B-R150-75	150	75	4.16	900	1.62	0.81	414	484
Beam-Column Test	BC-S150-150	150	150	4.22	900	1.58	1.58	405	484
	BC-R100-150	100	150	4.24	900	1.06	1.60	417	470
	BC-R75-150	75	150	4.16	900	0.81	1.62	414	484
	BC-R150-100	150	100	4.24	900	1.60	1.06	417	470
	BC-R150-75	150	75	4.16	900	1.62	0.81	414	484

Note:  $B$ =section width;  $D$ =section height;  $t$ =wall thickness of steel tube;  $L$ =specimen length or distance between fulcrums;  $\alpha_B$ ,  $\alpha_D$ =normalized width-thickness ratio;  $\sigma_{cy}$ =tensile yield strength;  $\sigma_{cu}$ =tensile strength.

#### Specimen

Compression test: C 0 - S 150 - 150

1 2 3 4 5

Bending test: B - S 150 - 150

1 3 4 5

1: Test (Concentric compression test, Eccentric compression test, Beam test, Beam-Column test)

2: Eccentricity (0mm, 25mm, 50mm)

3: Cross-section (Square, Rectangular)

4: Section width (150mm, 100mm, 75mm)

5: Section height (150mm, 100mm, 75mm)



## 2.2 Loading conditions

Figure 2 shows the loading conditions of the concentric and eccentric compression test. A universal testing machine with a capacity of 2 MN was used.

Figure 3 shows the loading conditions of the bending test. The beam test was performed using a 2 MN universal testing machine as shown in the Fig. 3(a). The beam-column test was performed using a 5 MN structural testing machine as shown in the Fig. 3(b).

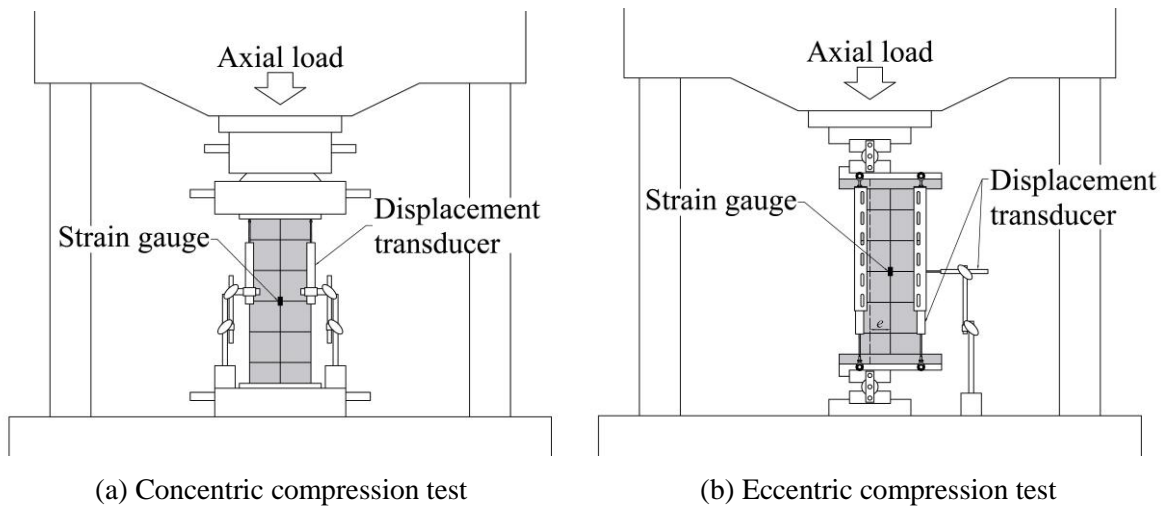


Fig.2. Loading conditions of compression test

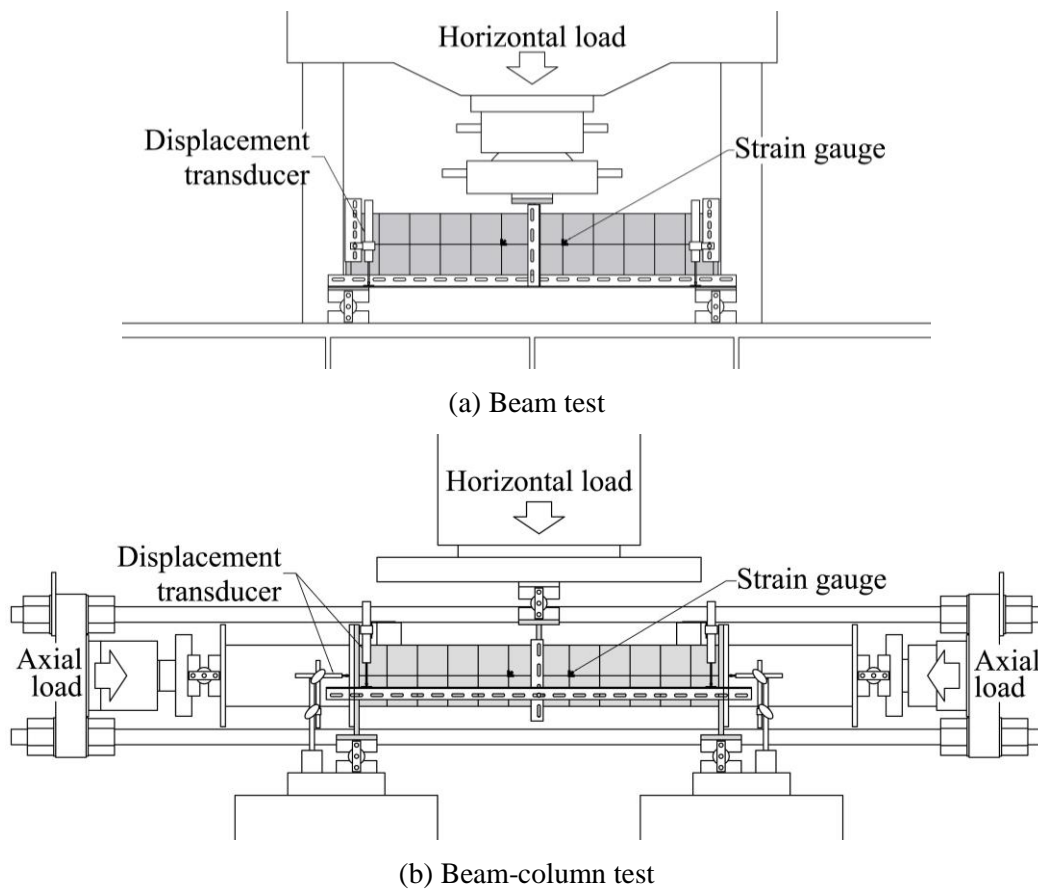


Fig. 3. Loading conditions of bending test



### 3. Compression test

Table 2 shows the results of the compression test.

When central compression was applied, the maximum axial load ( $N_{eu}$ ) reached near the yield load ( $N_{cy}$ ) for all the specimens regardless of the short-side length.

In the eccentric compression test, the effect of the difference in the short-side length could not be confirmed because the eccentric distance ( $e$ ) was set so that  $N_{eu}$  would be the same. However, the maximum moment ( $M_{eu}$ ) tended to increase as the short-side length became longer regardless of the bending direction. In the case of the same cross-section,  $M_{eu}$  was larger in the direction of the strong axis bending.

Table 2. Results of Compression Test

	Specimen	$B$ (mm)	$D$ (mm)	$t$ (mm)	$\sigma_{cy}$ (Mpa)	$N_{eu}$ (kN)	$N_{eu}/N_{cy}$	$M_{eu}$ (kN m)	$M_{eu}/M_{cu}$
Concentric Compression Test	C0-S150-150	150	150	4.22	405	951	0.97	-	-
	C0-R100-150	100	150	4.24	417	829	0.99	-	-
	C0-R75-150	75	150	4.16	414	700	0.96	-	-
Eccentric Compression Test	E50-S150-150	150	150	4.22	405	528	0.54	26.5	0.82
	E50-R100-150	100	150	4.24	417	481	0.58	24.9	0.98
	E50-R75-150	75	150	4.16	414	414	0.57	21.7	0.97
	E25-R150-100	150	100	4.24	417	539	0.65	14.1	1.01
	E25-R150-75	150	75	4.16	414	402	0.55	10.7	0.95

Note:  $N_{eu}$ =experimental maximum axial load;  $N_{cy}$ =tensile yield load;  $M_{eu}$ =experimental maximum moment;  $M_{cu}$ =theoretical ultimate moment.

Figures 4 and 5 show the relationship between the experimental axial load ( $N_e$ ) divided by the tensile yield load ( $N_{cy}$ ) and average axial strain  $\varepsilon$ .

In the central compression test, no difference was observed in the axial load–strain relationship owing to the difference in the cross-sectional shape.

On the strong axis of the eccentric compression test, the strain at the maximum load increased as the short-side length became shorter, as shown in the Fig. 5 (a). On the other hand, for the weak axis in the Fig. 5 (b), the effect of the short-side length was not observed on the strain at the maximum load.

Comparing the theoretical ultimate load ( $N_{cu}$ ) with the experimental  $N_{eu}$ , the square cross-section was slightly smaller than the calculated value, while, in the rectangular section,  $N_e$  was close to  $N_{cu}$ , especially for the test specimen with the short side of 100 mm. This tendency was observed on both the strong axis and the weak axis regardless of the bending direction.

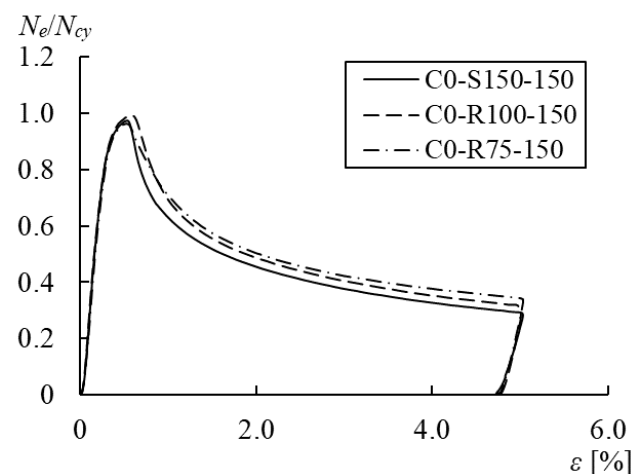


Fig. 4. Axial force-strain relationships in concentric compression test

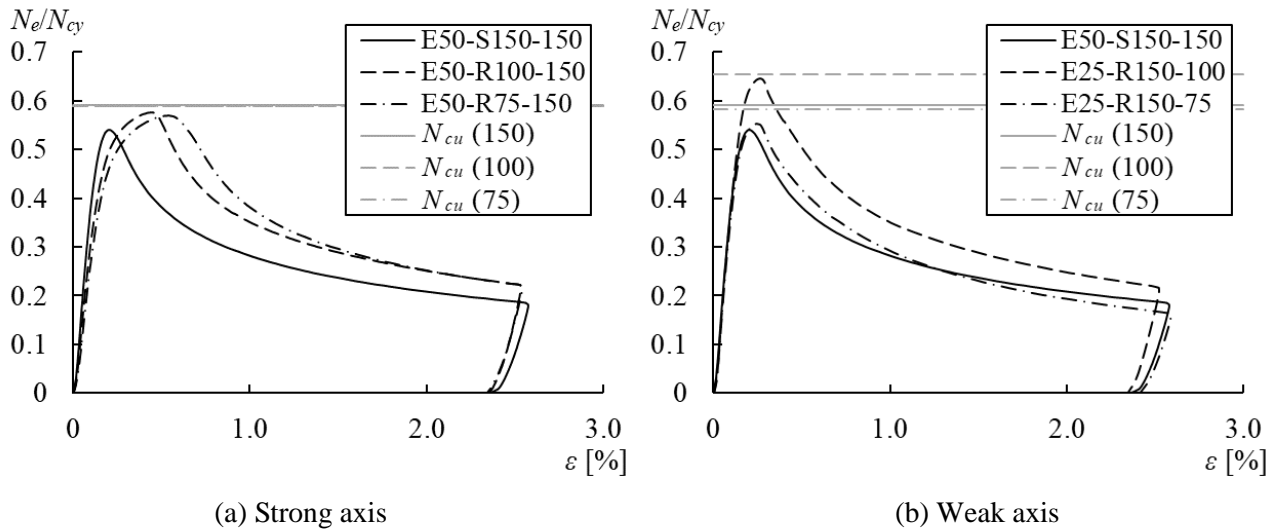


Fig. 5. Axial force-strain relationships in eccentric compression test

#### 4. Bending test

Table 3 shows the results of the bending test.

The maximum load ( $P_{eu}$ ), when the axial force was applied, was smaller than when there was no axial force regardless of the short-side length. The maximum load ( $P_{eu}$ ) and maximum moment ( $M_{eu}$ ) were affected by the geometrical moment of inertia, but  $M_{eu}/M_{cu}$  was affected by the width–height ratio of the cross-section. This tendency was observed with and without axial force.

Table 3. Results of Bending Test

	Specimen	$B$ (mm)	$D$ (mm)	$t$ (mm)	$\sigma_{cy}$ (Mpa)	$N_{20}$ (kN)	$P_{eu}$ (kN)	$M_{eu}$ (kN m)	$M_{eu}/M_{cu}$
Beam Test	B-S150-150	150	150	4.22	405	-	278	62.5	1.16
	B-R100-150	100	150	4.24	417	-	235	52.8	1.26
	B-R75-150	75	150	4.16	414	-	203	45.6	1.31
	B-R150-100	150	100	4.24	417	-	159	35.7	1.12
	B-R150-75	150	75	4.16	414	-	103	23.3	1.08
Beam-Column Test	BC-S150-150	150	150	4.22	405	196	238	53.5	1.06
	BC-R100-150	100	150	4.24	417	167	215	48.4	1.21
	BC-R75-150	75	150	4.16	414	146	185	41.6	1.25
	BC-R150-100	150	100	4.24	417	167	152	34.1	1.14
	BC-R150-75	150	75	4.16	414	146	95	21.4	1.07

Note:  $N_{20}$ = axial force ( $=0.20N_{cy}$ );  $P_{eu}$ =experimental maximum load;  $M_{eu}$ =experimental maximum moment;  $M_{cu}$ =theoretical ultimate moment.

Figure 6 shows the horizontal load-drift angle relationships in the beam test. The experimental drift angle is a value obtained by dividing the deflection by half of the distance between fulcrums. As for the deflection, a larger value was selected from the values measured by the displacement transducer installed at both ends of the test piece.



$P_{eu}/P_{cu}$  became larger as the short-side length became shorter on the strong axis, whereas,  $P_{eu}/P_{cu}$  became slightly smaller as the short-side length became shorter on the weak axis. After reaching the maximum load, the decrease in proof stress was smaller in the rectangular cross-section than in the square cross-section. The inclination of the elastic range was consistent for the three specimens on the strong axis but tended to decrease on the weak axis as the short-side length became shorter.

In the horizontal load-drift angle relationships in the beam-column test in the Fig. 7,  $P_{eu}/P_{cu}$  on the strong axis showed the same tendency as the beam test. The  $P_{eu}/P_{cu}$  of the weak axis became slightly smaller as the short-side length of the rectangular cross-section was shorter, but the square cross-section was at the lowest value.

There was no difference in  $P_{eu}/P_{cu}$  with or without axial force, but the decrease in the proof stress after reaching the maximum load was greater with the axial force. This is because local buckling generated in the compression-side steel plate progresses further when an axial force is applied

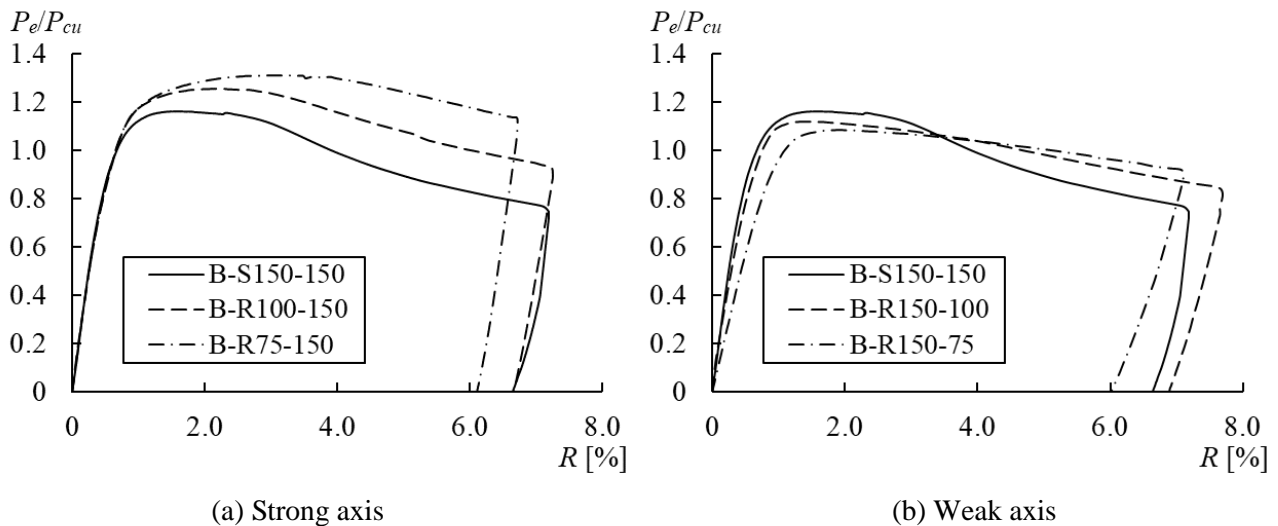


Fig. 6. Horizontal load-drift angle relationships in beam test

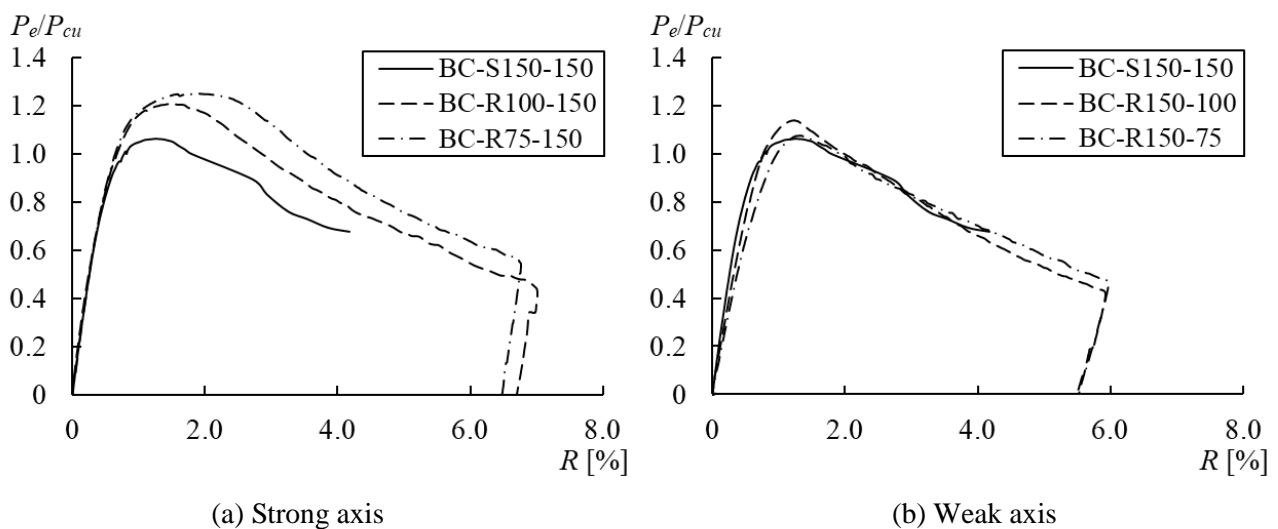


Fig. 7. Horizontal load-drift angle relationships in beam-column test



## 5. Conclusions

The main findings from the compression and bending test of rectangular steel tubes can be summarized as follows.

- 1) The load–strain relationship when concentric compression is applied is not affected by the short-side length.
- 2) In the eccentric compression test, only the strong axis was affected by the short-side length of the deformation capacity. The deformation under eccentric compression, therefore, is affected by the width–thickness ratio of the steel plate on the compression side.
- 3) The maximum load when a horizontal load is applied is affected by the section width–height ratio.
- 4) The decrease in proof stress when a horizontal load is applied increases due to the application of axial force.

## 6. References

- [1] Architectural Institute of Japan (AIJ). (2008): Recommendations for design and construction of concrete filled steel tubular structures. AIJ, Tokyo.
- [2] Fujimoto, T., Tanaka, H., Hirade, T., Takenaka, H. (2009): Design equation of rectangular CFT columns considering section shape. *AIJ J. Technol. Des.*, Vol. 15, No. 31, 757-760.
- [3] Miura, T., Fujimoto, T. (2019): Experimental study on bending compression behavior of rectangular steel tubes. *Kanto Chapter, AIJ*, Vol. 89, 521-524.
- [4] Miura, T., Fujimoto, T., Imai, K. (2019): Study on compression behavior of rectangular box-section members. *Summary of academic lecture, CIT, Nihon Univ.*, 5-8.
- [5] Imai, K., Fujimoto, T., Miura, T. (2019): Study on bending performance of rectangular box-section members. *Summary of academic lecture, CIT, Nihon Univ.*, 113-116.